The Seismic Record
A journal of the Seismological Society of America

Small Local Earthquake Detection Using Low-Cost MEMS Accelerometers: Examples in Northern and Central Italy

Valeria Cascone*[1], Jacopo Boaga[1], and Giorgio Cassiani[1]

Abstract

This study evaluates the seismicity detection efficiency of a new low-cost triaxial accelerometer prototype based on microelectromechanical systems (MEMS) technology. Networks of MEMS sensors were installed in telecommunication infrastructures to build two small arrays in northern and central Italy. The sensor prototypes recorded major earthquakes as well as nine small seismic events with $2.0 < M_L < 3.0$. Where possible, MEMS were compared to the closest high-quality seismic stations belonging to the national accelerometric network. The comparison, in terms of peak ground accelerations and spectral responses, confirms that the signals are in good agreement. The tested inexpensive MEMS sensors were able to detect small local events with epicentral distances as large as 50 km and provided an efficient characterization of the main motion parameters. This confirms that the proposed accelerometer prototypes are promising tools to integrate into traditional networks for local seismicity monitoring.

Cite this article as Cascone, V., Boaga, J., and Cassiani, G. (2021). Small Local Earthquake Detection Using Low-Cost MEMS Accelerometers: Examples in Northern and Central Italy. *The Seismic Record*. **1**, 20–26, doi: 10.1785/0320210007.

Supplemental Material

Introduction

Microelectromechanical systems (MEMS) sensors are miniaturized integrated circuit batch processing devices, with size ranging from a few micrometers to millimetres (Homeijer *et al.*, 2011). They are widely adopted in many industrial applications such as telecommunication, automotive, game controllers, and so on (Shi *et al.*, 2009). As a consequence of such widespread use, MEMS sensors are the most economic motion detector (Fleming *et al.*, 2009; Cochran *et al.*, 2012; D'Alessandro and D'Anna, 2013; Evans *et al.*, 2014; Lawrence *et al.*, 2014; Nof *et al.*, 2019). Moreover, the performance of MEMS sensors is rapidly growing, being already comparable to high-quality accelerometers (Kong *et al.*, 2016). Recent advances in micromachined sensors provide adequate sensitivity for measurement in geophysical applications. For example, several MEMS devices are suitable for volcanic activity studies (Andò *et al*, 2011), gravimetric and geodetic observations (Cenni *et al.*, 2019; Mustafazade *et al.*, 2020), and seismological and earthquake engineering projects (Holland, 2003; Cochran *et al.*, 2012). These sensors can reach an efficient performance for moderate ($5.0 > M_w > 5.9$) to large ($M_w > 6.0$) earthquake detection at distances on the order of tens of kilometres (Boaga *et al.*, 2019; Liu *et al.*, 2011). Because of the low cost of the MEMS motion sensors (~ two orders of magnitude less than a classical high-quality seismological stations), they could be adopted for the installation of dense accelerometric networks. Ground-motion wavefield recording is limited to relatively coarse spatial sampling due to a limited number of installed sensors and large instrument spacing (on the order of tens of kilometres). This can lead to spatial aliasing of the wavefield and consequently an underestimation of the effective peak ground acceleration (PGA) as well as uncertainties in the estimation of local effects on the resulting shake maps (Wald *et al.*, 2008). These are the reasons why several

1. Department of Geosciences, University of Padova, Padova, Italy, https://orcid.org/0000-0001-7402-0985 (VC); https://orcid.org/0000-0001-8588-3962 (JB)

*Corresponding author: valeria.cascone@phd.unipd.it

dense low-cost MEMS networks have been recently tested for the monitoring of strong earthquakes ground shaking (Cochran *et al.*, 2009; Lawrence *et al.*, 2014). The question remains whether such technology is suitable for low-magnitude seismicity detecting. In particular, an interesting use of these sensors could be the monitoring of possible induced seismicity, an issue of growing public concern in face of some of the practices in the energy industry (oil and gas production, gas and CO_2 storage, geothermic operations, Valoroso *et al.*, 2009; Clarke *et al.*, 2014). Induced seismicity usually generates moderate seismic events of magnitude rarely larger than 3.0 (Ellsworth, 2013; Westaway and Younger, 2014; Walsh and Zoback, 2015; Weingarten *et al.*, 2015). For most of the national regulations, reaching magnitude values of the order of $M_w = 3.0$ puts operations at risk. Most of the induced earthquakes recorded in the world are of $M_w < 3$ and often much lower, but this may nevertheless trigger the public concern that larger events may follow (e.g., Majer *et al.*, 2007). As a consequence, subsoil activities must provide a suitable seismic monitoring plan that involves the installation of an expensive network of sensors. The use of advanced MEMS low-cost sensors could greatly improve these applications, freeing resources on one hand and providing better monitoring on the other.

In this study, we tested the performance of a MEMS sensor prototype designed by the Italian company ADEL srl to monitor small local events. A selection of these sensors that are digital, multirange, triaxial MEMS accelerometers (named ASX1000) were installed in seismic zones of northern and central Italy, to evaluate their performance in recording low-energy events.

We performed an analysis of the detected seismicity ($M_L < 3.0$), comparing the data as recorded by the MEMS sensors with the nearest available high-quality accelerometers managed by the Italian National Protection Service (Rete Accelerometrica Nazionale [RAN]). The results are promising and open new perspectives for the extensive use of such low-cost MEMS sensors for the monitoring of local seismicity.

Methodology

The MEMS sensor prototype adopted in this work (Adel ASX1000) is a triaxial MEMS accelerometer, with an internal circuit of transduction and digital output. The sensor has three sensing elements oriented along mutually orthogonal axes. It operates in high sensitivity mode for an acceleration range of $\pm 2g$ ($g = 9.80665$ m/s^2). The prototype frequency bandwidth is set to 0–62.5 Hz at 250 Hz sampling. ASX1000 has a micro-SD memory card that stores the recorded data and three

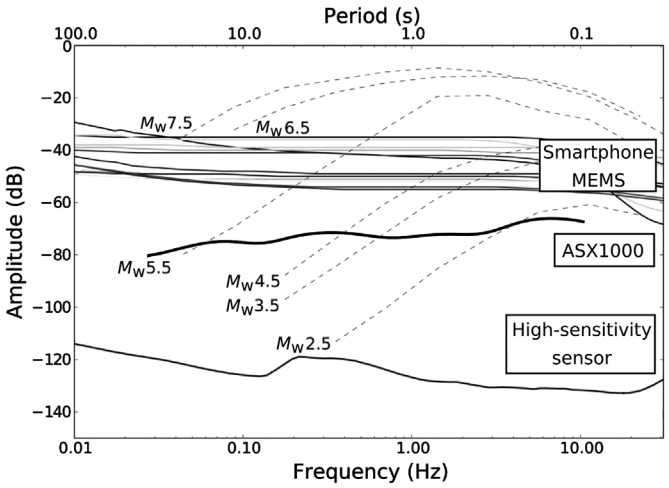

Figure 1. Noise floor of the ASX1000 microelectromechanical systems (MEMS) prototype compared to the most common smartphone MEMS sensors and high-quality force balance instruments. Dashed black lines are typical ground-motion amplitudes of earthquakes measured at 10 km from the epicenter for various magnitudes (from Kong *et al.*, 2016, modified).

communication channels for the remote control and data transmission (a serial channel RS-422 or RS485, a LAN Ethernet 10/100 Mbit/s, and an USB 2.0). The MEMS sensor prototype was calibrated in the laboratory on a shake table with a sweeping signal characterized by a frequency range between 0 and 100 Hz, a duration of 60 s, and a maximum amplitude of ± 0.2 m/s^2. The prototype proved to be in very good agreement with the laser motion reference for the frequency response up to 80 Hz. Noise analysis of the single components detects a power spectral density (PSD) with a general downward trend between −80 and −65 dB in the 0.2–10 Hz frequency range, interesting for earthquake engineering (Fig. 1). Figure 1 compares the detectable magnitude of seismic events measured at distances of 10 km, as in Kong *et al.* (2016), with the obtained PSD from the horizontal component of the ASX1000 MEMS prototype, common industrial phone MEMS sensors, and seismological high-quality stations. Lab tests suggested that ASX1000 has the potential sensitivity to record local events with magnitude $M_w > 2.5$ in the 2–10 Hz frequency range, which is the most critical frequency range of seismological interest.

To test the performance in detecting small seismic events, 15 ASX1000 prototypes were installed at two seismic active areas of Italy: the inner part of the Umbria Valley (central Italy, Chiaraluce *et al.*, 2017) and the southern-east Alpine Front (northern Italy, Galadini *et al.*, 2005). Figure 2 shows

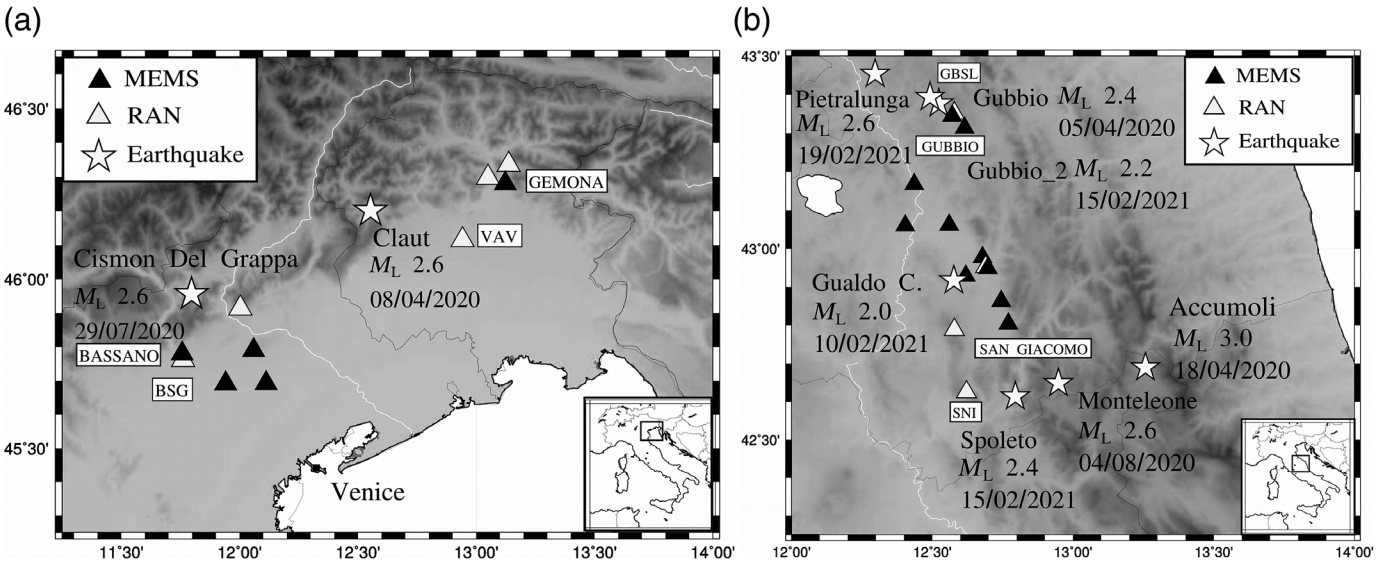

Figure 2. MEMS sensors arrays in (a) northern and (b) central Italy. Black triangles are the MEMS accelerometers, the white triangles are the high-quality available stations. The stars represent the epicenters with $M_L < 3$ discussed in this study. The insets display the Italian Peninsula with black squares, representing the selected study areas.

the locations of the MEMS arrays, the locations of the closest national strong-motion high-quality sensors (RAN that use Kinemetrics Episensor ES-T sensors), and the epicenters of the recorded seismic events analyzed in this study. The MEMS sensors were installed inside telecommunication infrastructures at the base of the local server room, and the sensors were firmly coupled with the ground with screws and plugs. Raw data were transmitted to a central service in real time through a LAN connection.

Results

The MEMS sensors were able to detect nine small local earthquakes with $2.0 < M_L < 3.0$ between April 2020 and February 2021. The corresponding epicenters are shown in Figure 2. The location and the local magnitude of the recorded events were retrieved from the National Seismic Institute earthquakes database (Istituto Nazionale di Geofisica e Vulcanologia [INGV]). Figure 3 shows the time series signal as recorded by the ASX1000 MEMS prototypes (horizontal-transverse component), the earthquake's ID name, and the distance between the sensors and the epicenters.

Even small events are clearly visible, especially for the nearest epicenters (e.g., Gubbio, Gualdo C., and Gubbio_2 earthquakes in Fig. 3a,f,h, respectively). From the recorded waveforms, we determined the PGA values and the acceleration response spectra (5% damped spectral acceleration [SA]), to be compared with the recordings of the high-quality stations belonging to the RAN. The RAN accelerograms can be downloaded from the Italian Civil Protection website (see Data Availability Statement). Figure 4 shows a comparison between the horizontal-transverse components recorded by our MEMS stations and by the high-quality accelerometers for the events having similar epicentral distances and soil conditions; this comparison avoids, as much as possible, unreliable comparison due especially to local effects (e.g., stations installed on hard rock vs. soft sediments). The considered events were named Gubbio, Cismon, Claut, and Pietralunga, as recorded respectively by the MEMS Gubbio, Bassano, Gemona, and the high-quality stations GBSL, BSG, and VAV (see Fig. 2).

As apparent from Figure 4, MEMS recordings are in very good agreement with the high-quality stations, both in terms of PGA and spectral response, especially for the closest events (consider the Gubbio–GBSL stations comparison in Fig. 4a).

In Table 1, we report the PGA values as recorded by the ASX1000 MEMS prototypes and by the closest high-quality RAN seismic stations for the earthquakes considered in Figure 4 along with the station–event distances, the MEMS–RAN distances (interstation distances), and the discrepancy of the PGAs ($\Delta PGAs = PGA_{MEMS} - PGA_{RAN}$).

The PGA values are very similar, especially for the horizontal components, presenting an average discrepancy between MEMS sensors and high-quality accelerometers of <15%.

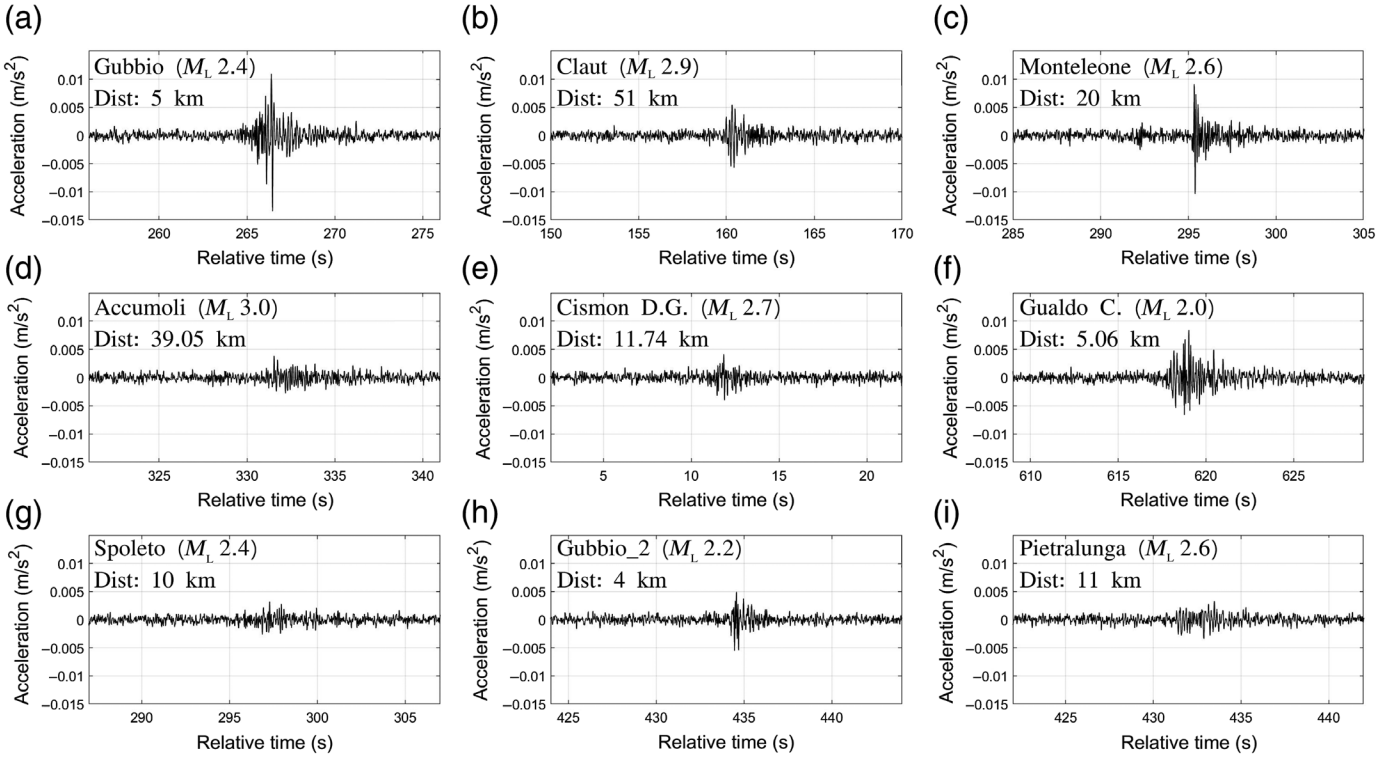

Figure 3. Time series of the seismic events as recorded by the horizontal component of the ASX1000 MEMS prototype. Each panel shows the event name, the estimated local magnitude M_L, and the sensor–event distance. (a) Gubbio earthquake; (b) Claut earthquake; (c) Monteleone earthquake; (d) Accumoli earthquake; (e) Cismon earthquake; (f) Gualdo C. earthquake; (g) Spoleto earthquake; (h) Gubbio_2 earthquake; and (i) Pietralunga earthquake (see Fig. 2 for locations; and for details, see Data Availability Statement).

The best match between the two sensors is given by the Gubbio earthquake recordings in which the high-quality station RAN and the MEMS sensor have nearly the same location. In this case discrepancy is ~6%. Higher discrepancy is observed for the vertical component (Z) of the Gubbio–GBSL stations, possibly related to installation issues. The ASX1000 MEMS responds in agreement with high-quality stations even for remote and small earthquakes, such as the case of the Claut event (with the epicenter 51 km away from the recording stations).

Discussion and Conclusions

MEMS sensors are often used to detect strong-motion events. Our tests show the reliability of MEMS also for low magnitude ($2.0 < M_L < 3.0$) seismicity monitoring. This study investigates the performance of the low-cost ASX1000 MEMS prototype accelerometer under small earthquake ($M_L < 3.0$) excitation. Sensors have been initially tested using a calibrated shake table. Under the controlled sweep excitation, the MEMS sensor shows a good performance in the frequencies up to 80 Hz, critical for the earthquake engineering aims, and the self-noise test shows that the PSD is around −80 dB in the 0.2–10 Hz range. Our field results show that the low-cost ASX1000 MEMS prototypes are suitable to record seismic events with a minimum local magnitude of $M_L = 2.0$ and epicentral distance <20 km or $M_L \sim 3$ at 50 km distance. The comparison of the PGA and spectral responses inferred from our MEMS sensors and the nearest high-quality accelerometers (belonging to the RAN) yields a good match, especially at smaller epicenter distances and when the interstation distances (MEMS–RAN) are lower than 2 km.

We note that these sensors are installed in urban telecommunication infrastructures. Although they are located in a noisy environment, not intended for seismic monitoring, they are still capable of recording small local earthquakes.

The use of low-cost sensors for small or local earthquakes monitoring will allow the development of dense accelerometric networks, thus mitigating the spatial sampling issues and providing highly detailed ground shaking maps, even for small

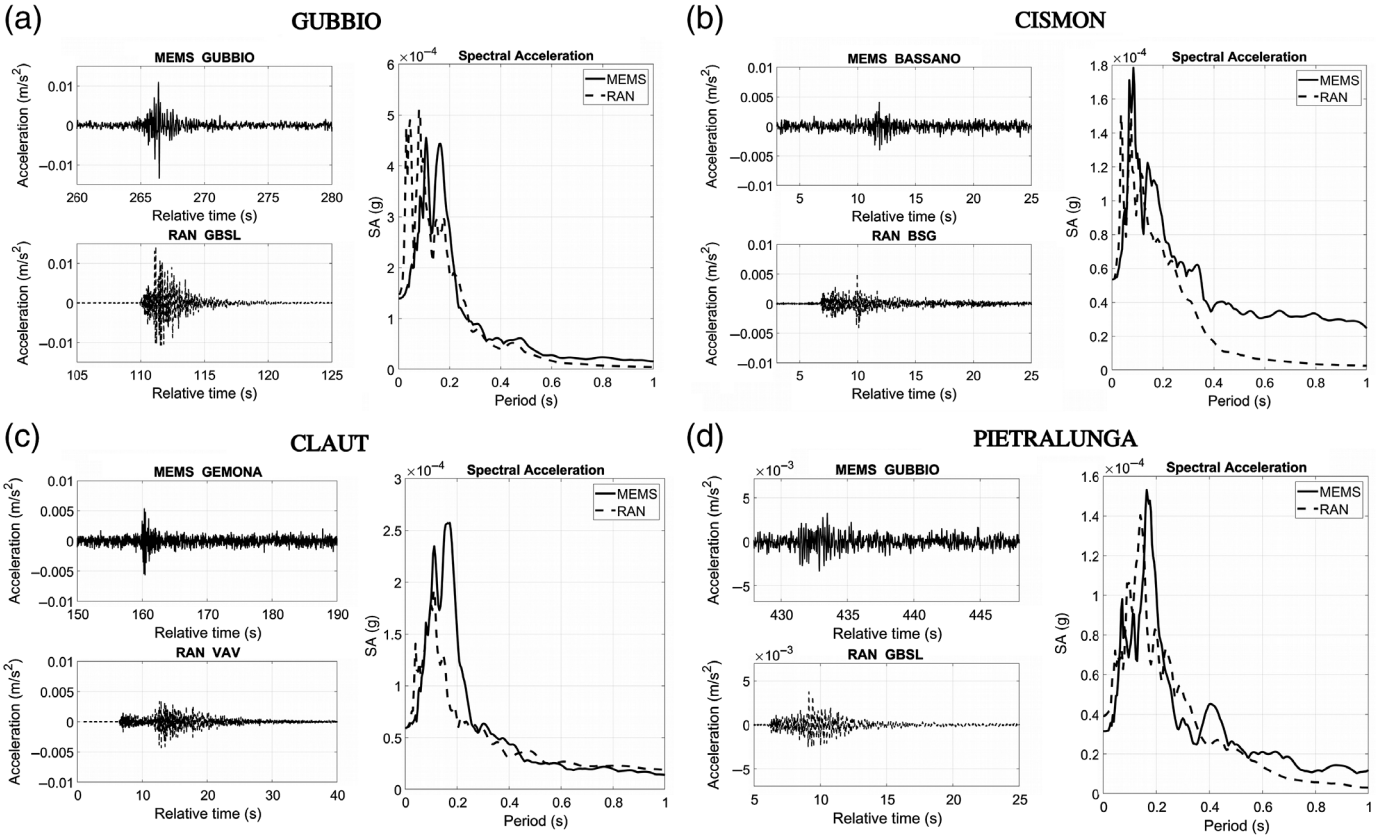

Figure 4. Acceleration time histories and corresponding normalized response spectra for both the MEMS stations and the RAN high-quality stations. For each event, the MEMS signal is shown above (solid line) and RAN signal below (dashed line). In the spectra plots, solid lines are the MEMS response and dashed lines are RAN response spectra. Events: (a) Gubbio, (b) Cismon, (c) Claut, and (d) Pietralunga.

events that are of course also very frequent. A well-defined shaking pattern inferred from small earthquakes can help identify local site effects that are often overlooked.

On the basis of these results, the ASX1000 MEMS prototype could be efficiently integrated into existing national seismic networks (as suggested by D'Alessandro *et al.*, 2019).

Moreover, the MEMS sensor prototype evaluated in this study could potentially be adopted for induced seismicity detection. A dense network with MEMS sensors distributed in the immediate proximity of industrial activity sites (such as oil and gas production, geothermic operation, etc.) could improve low-magnitude seismicity monitoring.

While a promising geophysical tool, the low-cost ASX1000 prototype still suffers from a high level of internal noise, which is usually considered to limit their use for several seismological purposes, such as accurate earthquake locations or origin time estimations. Nevertheless, the fast improvement of sensors quality combined with decreasing costs suggests that in the near future MEMS-based motion networks will play a relevant role in the monitoring of lower-level seismicity, which still conveys important seismologic information such as local seismic response to large, destructive events.

Data and Resources

Data availability statement: The public data used in this article are available at http://ran.protezionecivile.it and http://terremoti.ingv.it/. Other data are available upon request for scientific purposes.

The microelectromechanical systems (MEMS) data supporting the conclusions of this article, being property of a private company, is made available by the authors only upon request for scientific purposes. The Rete Accelerometrica Nazionale (RAN) accelerometric data are public and can be downloaded from the Italian Civil Protection website (http://ran.protezionecivile.it, available only for earthquakes with $M_L \geq 2.5$, and only upon request for smaller M_L). The event locations and timing are public data and can be downloaded from the National Institute of Geophysics and Volcanology

Table 1
Selected Earthquakes for the Comparison between the Microelectromechanical Systems (MEMS) Sensors and Rete Accelerometrica Nazionale (RAN) High-Quality Stations

Earthquakes ID, Date, Time (yyyy/mm/dd hh:mm:ss, UTC)	M_L	PGA MEMS (m/s^2)	PGA RAN (m/s^2)	Event–MEMS Distance (km)	Event–RAN Distance (km)	Interstation Distance (km)	ΔPGAs (m/s^2)
GUBBIO, 2020/04/05 14:33:48 (X comp)	2.4	0.0134	0.0143	5.5	5	0.5	−0.0009
GUBBIO, 2020/04/05 14:33:48 (Y comp)	2.4	0.0086	0.0119	5.5	5	0.5	−0.0033
GUBBIO, 2020/04/05 14:33:48 (Z comp)	2.4	0.0073	0.0110	5.5	5	0.5	−0.0037
CLAUT, 2020/04/08 15:10:46 (X comp)	2.9	0.0057	0.0042	51	38.1	34.9	0.0015
CLAUT, 2020/04/08 15:10:46 (Y comp)	2.9	0.0056	0.0047	51	38.1	34.9	0.0009
CLAUT, 2020/04/08 15:10:46 (Z comp)	2.9	–	–	51	38.1	34.9	–
CISMON, 2020/07/29 22:26:34 (X comp)	2.7	0.0041	0.0052	20	19.1	2	−0.0011
CISMON, 2020/07/29 22:26:34 (Y comp)	2.7	0.0032	0.0034	20	19.1	2	−0.0002
CISMON, 2020/07/29 22:26:34 (Z comp)	2.7	0.0044	0.0042	20	19.1	2	0.0002
PIETRALUNGA, 2021/02/19 23:42:45 (X comp)	2.6	0.0034	0.0037	11	5	0.5	−0.0003
PIETRALUNGA, 2021/02/19 23:42:45 (Y comp)	2.6	0.0033	0.0030	11	5	0.5	0.0003
PIETRALUNGA, 2021/02/19 23:42:45 (Z comp)	2.6	0.0039	0.0024	11	5	0.5	0.0015

Columns 2–8 show the local magnitude (M_L); peak ground acceleration (PGA) recorded by MEMS and RAN sensors; distances between the MEMS sensors and epicenters; distances between RAN stations and epicenters; interstation (RAN MEMS) distances; ΔPGA that is the difference between the PGAs recorded by MEMS and RAN sensors ($PGA_{MEMS} - PGA_{RAN}$).

(INGV) website (http://terremoti.ingv.it/). All websites were last accessed in February 2021. Supplemental material for this article includes the complete technical information of the MEMS sensor prototype and the calibration experiment on the shake table.

Declaration of Competing Interest

The authors declare no conflict of interest.

Acknowledgments

The authors wish to thank ADEL srl for the use of their proprietary data and TIM SpA for the permission granted to microelectromechanical systems (MEMS) installation in their infrastructures. The authors would also like to thank David Zuliani of the Seismological Research Center of Istituto Nazionale di Oceanografia e Geofisica Sperimentale (OGS) for the calibration experiment on the shake table apparatus.

References

Andò, B., S. Baglio, G. L'Episcopo, V. Marletta, N. Savalli, and C. Trigona (2011). A BE-SOI MEMS for inertial measurement in geophysical applications, *IEEE Trans. Instrum. Meas.* **60,** no. 5, 1901–1908.

Boaga, J., F. Casarin, G. De Marchi, M. R. Valluzzi, and G. Cassiani (2019). 2016 central Italy earthquakes recorded by low-cost MEMS-distributed arrays, *Seismol. Res. Lett.* **90,** no. 2A, 672–682.

Cenni, N., J. Boaga, F. Casarin, G. D. Marchi, M. R. Valluzzi, and G. Cassiani (2019). 2016 Central Italy Earthquakes: Comparison between GPS signals and low-cost distributed MEMS arrays, *Adv. Geosci.* **51,** 1–14.

Chiaraluce, L., R. Di Stefano, E. Tinti, L. Scognamiglio, M. Michele, E. Casarotti, M. Cattaneo, P. De Gori, C. Chiarabba, G. Monachesi, *et al.* (2017). The 2016 central Italy seismic sequence: A first look at the mainshocks, aftershocks, and source models, *Seismol. Res. Lett.* **88,** no. 3, 757–771.

Clarke, H., L. Eisner, P. Styles, and P. Turner (2014). Felt seismicity associated with shale gas hydraulic fracturing: The first documented example in Europe, *Geophys. Res. Lett.* **41,** no. 23, 8308–8314.

Cochran, E. S., J. F. Lawrence, C. Christensen, and R. S. Jakka (2009). The quake-catcher network: Citizen science expanding seismic horizons, *Seismol. Res. Lett.* **80,** no. 3, 26–30.

Cochran, E. S., J. F. Lawrence, A. Kaiser, B. Fry, A. Chung, and C. Christensen (2012). Comparison between low-cost and traditional

MEMS accelerometers: A case study from the M7. 1 Darfield, New Zealand, aftershock deployment, *Ann. Geophys.* **54,** no. 6, doi: 10.4401/ag-5268.

D'Alessandro, A., and G. D'Anna (2013). Suitability of low-cost three-axis MEMS accelerometers in strong-motion seismology: Tests on the LIS331DLH (iPhone) accelerometer, *Bull. Seismol. Soc. Am.* **103,** no. 5, 2906–2913.

D'Alessandro, A., A. Costanzo, C. Ladina, F. Buongiorno, M. Cattaneo, S. Falcone, C. La Piana, S. Marzorati, S. Scudero, G. Vitale, *et al.* (2019). Urban seismic networks, structural health and cultural heritage monitoring: The national earthquakes observatory (INGV, Italy) experience, *Front. Built Environ.* **5,** 127.

Ellsworth, W. L. (2013). Injection-induced earthquakes, *Science* **341,** no. 6142, doi: 10.1126/science.1225942.

Evans, J. R., R. M. Allen, A. I. Chung, E. S. Cochran, R. Guy, M. Hellweg, and J. F. Lawrence (2014). Performance of several low-cost accelerometers, *Seismol. Res. Lett.* **85,** 147–158, doi: 10.1785/0220130091.

Fleming, K., M. Picozzi, C. Milkereit, F. Kuhnlenz, B. Lichtblau, J. Fischer, C. Zulfikar, and O. Ozel (2009). The self-organizing seismic early warning information network (SOSEWIN), *Seismol. Res. Lett* **80,** no. 5, 755–771.

Galadini, F., M. E. Poli, and A. Zanferrari (2005). Seismogenic sources potentially responsible for earthquakes with M ≥ 6 in the eastern Southern Alps (Thiene-Udine sector, NE Italy), *Geophys. J. Int.* **161,** no. 3, 739–762.

Holland, A. (2003). Earthquake data recorded by the MEMS accelerometer: Field testing in Idaho, *Seismol. Res. Lett.* **74,** no. 3, 20–26.

Homeijer, B., D. Lazaroff, D. Milligan, R. Alley, J. Wu, M. Szepesi, B. Bicknell, Z. Zhang, R. G. Walmsley, and P. G. Hartwell (2011). Hewlett packard's seismic grade MEMS accelerometer, *2011 IEEE 24th International Conf. on Micro Electro Mechanical Systems*, IEEE, 585–588.

Kong, Q., R. M. Allen, L. Schreier, and Y. W. Kwon (2016). MyShake: A smartphone seismic network for earthquake early warning and beyond, *Sci. Adv.* **2,** no. 2, e1501055, doi: 10.1126/sciadv.1501055.

Lawrence, J. F., E. S. Cochran, A. Chung, A. Kaiser, C. M. Christensen, R. Allen, J. W. Baker, B. Fry, T. Heaton, D. Kilb, *et al.* (2014). Rapid earthquake characterization using MEMS accelerometers and volunteer hosts following the M 7.2 Darfield, New Zealand, earthquake, *Bull. Seismol. Soc. Am.* **104,** no. 3, 184–192.

Liu, C. M., B. C. Chou, R. C. F. Tsai, N. Y. Shen, B. S. Chen, E. C. Cheng, H. C. Tuan, A. Kalnitsky, S. Cheng, C. H. Lin, *et al.* (2011). MEMS technology development and manufacturing in a CMOS foundry, *2011 16th International Solid-State Sensors, Actuators and Microsystems Conf.*, IEEE, 807–810.

Majer, E. L., R. Baria, M. Stark, S. Oates, J. Bommer, B. Smith, and H. Asanuma (2007). Induced seismicity associated with enhanced geothermal systems, *Geothermics* **36,** no. 3, 185–222.

Mustafazade, A., M. Pandit, C. Zhao, G. Sobreviela, Z. Du, P. Steinmann, X. Zou, R. T. Howe, and A. A. Seshia (2020). A vibrating beam MEMS accelerometer for gravity and seismic measurements, *Sci. Rep.* **10,** no. 3, 1–8.

Nof, R. N., A. I. Chung, H. Rademacher, L. Dengler, and R. M. Allen (2019). MEMS Accelerometer Mini-Array (MAMA): A low-cost implementation for earthquake early warning enhancement, *Earthq. Spectra* **35,** no. 3, 21–38.

Shi, G., C. S. Chan, W. J. Li, K. S. Leung, Y. Zou, and Y. Jin (2009). Mobile human airbag system for fall protection using MEMS sensors and embedded SVM classifier, *IEEE Sensor J.* **9,** no. 5, 495–503.

Valoroso, L., L. Improta, L. Chiaraluce, R. Di Stefano, L. Ferranti, A. Govoni, and C. Chiarabba (2009). Active faults and induced seismicity in the Val d'Agri area (southern Apennines, Italy), *Geophys. J. Int.* **178,** no. 3, 488–502.

Wald, D., K. W. Lin, K. Porter, and L. Turner (2008). ShakeCast: Automating and improving the use of ShakeMap for post-earthquake decision-making and response, *Earthq. Spectra* **24,** no. 2, 533–553.

Walsh, F. R., and M. D. Zoback (2015). Oklahoma's recent earthquakes and saltwater disposal, *Sci. Adv.* **12,** no. 5, e1500195, doi: 10.1126/sciadv.1500195.

Weingarten, M., S. Ge, J. W. Godt, B. A. Bekins, and J. L. Rubinstein (2015). High-rate injection is associated with the increase in US mid-continent seismicity, *Science* **348,** no. 6241, 1336–1340.

Westaway, R., and P. L. Younger (2014). Quantification of potential macroseismic effects of the induced seismicity that might result from hydraulic fracturing for shale gas exploitation in the UK, *Q. J. Eng. Geol. Hydrogeol* **47,** no. 4, 333–350.

Manuscript received 20 March 2021
Published online 13 May 2021